

THE GALAXY CLUSTER EVOLUTION SURVEY (GLACE): OVERVIEW AND STATUS REPORT

M. Sánchez-Portal,¹ I. Pintos-Castro,^{2,3} R. Pérez-Martínez,¹ J. Cepa,^{2,3} A. Bongiovanni,^{2,3} A. Ederoclite,^{2,3} A. M. Pérez García,^{2,3} J. I. González-Serrano,⁴ E. J. Alfaro⁵ and the GLACE Team

RESUMEN

El cartografiado GLACE tiene como objeto construir mapas de importantes líneas de emisión en varios cúmulos de galaxias a $z \sim 0.40$, 0.63 y 0.85 , mediante los filtros sintonizables (TF) del instrumento OSIRIS. Este estudio está encaminado a responder a preguntas clave sobre los procesos físicos que actúan en las galaxias en el curso del crecimiento jerárquico de los cúmulos.

ABSTRACT

Aimed at understanding the evolution of galaxies in clusters, the GLACE survey is mapping a set of key optical lines in several galaxy clusters at $z \sim 0.40$, 0.63 and 0.85 , using the Tunable Filters (TF) of the OSIRIS instrument. This study will address key questions about the physical processes acting upon the infalling galaxies during the course of hierarchical growth of clusters.

Key Words: galaxies: active — galaxies: clusters: individual: (ZwCl0024+1654) — galaxies: star formation

1. INTRODUCTION

It is well known that, while the cores of nearby clusters are dominated by red early-type galaxies, a significant increase in the fraction of cluster blue galaxies is observed at $z > 0.2$ (the so-called Butcher-Oemler –BO– effect; Butcher & Oemler 1984). An equivalent increase in obscured star formation (SF) activity has also been seen in mid- and far-IR surveys of distant clusters (Haines et al. 2009; Pereira et al. 2010) as well as a growing population of AGN. In fact, the mass-normalized cluster SFR has been found to decline rapidly since $z \sim 1$ as $\propto (1+z)^6$ (e.g. Koyama et al. 2011). Even focusing on a single epoch, aspects of this same evolutionary trend have been discovered in the outer parts of clusters where significant changes in galaxy properties can be clearly identified (color, spectral properties, morphology). In a hierarchical model of structure formation, galaxies merge into larger and larger systems as time progresses. It is quite likely that this accretion process is responsible for a transformation of the properties of cluster galaxies both as a function of redshift and as a function of environment (Balogh et al. 2000), but the physical mechanisms responsible for these evolutionary and environmental transformations are uncertain (e.g. ram-pressure stripping,

tidal truncation, harassment, merging, etc.; Treu et al. 2003). The physical processes proposed above act on the cluster population of emission line galaxies (ELG; comprising SF and AGN population); narrow-band imaging surveys are very efficient to identify *all* the ELG in a cluster. “Classical” narrow-band imaging surveys have demonstrated to be a powerful tool, but suffer from ambiguity about the true fluxes of detected sources and do not provide either accurate membership or dynamical information about the population.

2. SURVEY OBJECTIVES

Overcoming the limitations of traditional narrow-band surveys explained above, GLACE has been designed as an ambitious and innovative survey of ELG and AGN in a well-studied and well-defined sample of clusters in three narrow redshift windows, chosen to be relatively free of strong sky emission lines. This program is undertaking a panoramic census of SF and AGN activity within several clusters at $z \sim 0.40$, 0.63 and 0.85 , mapping a set of important lines: $H\alpha$ (only at $z \sim 0.4$), $H\beta$, $[\text{OII}]3727$ and $[\text{OIII}]5007$; these maps of ELG are compared with the structures of these systems (as traced by galaxies, gas and dark matter) to address several crucial issues: (i) Star formation in clusters: We will determine how the star formation properties of galaxies relate to their position in the large scale structure. This will provide a key diagnostic to test between different models for the environmental influence on galaxy evolution. We are mapping the extinction-

¹ESAC/INSA, P.O. Box 78, 28629 Villanueva de la Cañada, Madrid, Spain (miguel.sanchez@sciops.esa.int).

²IAC, La Laguna, Tenerife, Spain.

³Dep. de Astrofísica, ULL, Tenerife, Spain.

⁴IAA, CSIC, Granada, Spain.

⁵IFCA, CSIC-UNICAN, Santander, Spain.

corrected star formation through $H\alpha$ and $[OII]$, over a large and representative region in a statistically useful sample of clusters. The survey has been designed to reach $SFR \sim 2 M_{\odot} \text{ yr}^{-1}$ (i.e. below that of the Milky Way) with 1 magnitude of extinction at $H\alpha$ ⁶. (ii) The role of AGNs: Whether the fraction of AGN is environment-dependent or not is a matter of debate: while some results (e.g. Miller et al. 2003) point towards a lack of dependency of the AGN fraction with the local galaxy density, other authors (e.g. Kauffmann et al. 2004) conclude that high-luminosity AGN do avoid high-density regions. Such a lack of AGN in clusters, as compared to the field, may be related to the evolution of galaxies as they enter the cluster environment. (iii) The study of the distribution of galaxy metallicities with cluster radii is another potentially powerful mean to investigate evolution within clusters. As galaxies fall into clusters and travel toward the cluster center along their radial orbits, they interact with the intra-cluster medium (ICM) and other cluster galaxies, thus getting progressively stripped of their gas reservoir. GLACE will allow to derive extinction-corrected metallicities using standard line diagnostics (N2, R23, O3N2). The survey can address many other interesting topics: for instance the cluster accretion history can be traced by studying the census of ELGs at different cluster-centric distances. In addition, the survey will provide an accurate assessment of cluster membership, without the need of a spectroscopic follow-up.

3. SURVEY IMPLEMENTATION, STATUS AND FIRST RESULTS

Regarding the technical implementation, the GLACE survey applies the technique of TF tomography: for each line, a set of images are taken through the OSIRIS TF, each image tuned at a different wavelength (equally spaced), so that a rest frame velocity range of several thousands km s^{-1} (6500 km s^{-1} for our first target) centred at the mean cluster redshift is scanned for the full TF field of view of 8 arcmin in diameter. Additional images are taken to compensate for the blueshift of the wavelength from centre to the edge of the field of view. Finally, for each pointing and wavelength tuned, three dithered exposures allow correcting for etalon diametric ghosts, using combining sigma clipping algorithms. The TF FWHM and sampling allows to deblend the $H\alpha$ and N II lines with with an accuracy better than 3%. The chosen parameters allow a continuum subtraction accuracy better than 2% and a

⁶ $f_{H\alpha} = 1.89 \times 10^{-16} \text{ erg s}^{-1}$ at $z=0.4$ using standard SFR-luminosity conversion factors (Kennicutt 1998).

photometric accuracy better than 6%. We have required to cover $\simeq 2$ Virial radii (some 4 Mpc) within the targeted clusters.

The first target chosen for the GLACE survey was the rich cluster ZwC10024+1654 at $z=0.395$; this object has been comprehensively studied, from X-ray to FIR so we had a wealth of ancillary data at our disposal. The observations of this cluster have been implemented in regular Spanish open time (CAT) and OSIRIS guaranteed time. The second target, the cluster RX J1257.2+4738 at $z=0.86$ (Ulmer et al. 2009) was approved as ESO/GTC program (72 dark hours allocated) in period 86B. Unfortunately, the observations have progressed little at the time of writing this contribution so no results can be shown at present. A third target, the young, massive cluster XLSSC03 at $z=0.839$ has been proposed to ESO for period 89B. We plan to issue regular open time proposals to observe a second cluster at $z\sim 0.4$ and two targets in the intermediate redshift bin, $z\sim 0.63$.

Here we present results from the processing of the $H\alpha/N II$ line complex in the central pointing of the cluster ZwC10024+1654. (5.15 hours of on-source integration time, covering the 9047–9341 Å range in 50 scan steps). Data reduction was performed using a customized version of the TFRED package (Jones et al. 2002) and private IDL scripts. Details of the processing are given in Sánchez-Portal et al. (in preparation).

From the raw catalog of 933 sources detected at $>3\sigma$ in the deep image, 722 are detected in all spectral scans. From these, 89 very robust (i.e. high S/N) ELG have been further selected. Examples of pseudo-spectra built from the TF scans are shown in Figure 1. We have cross-matched our ELG catalog with a public photometric and spectroscopic catalog (Moran et al. 2007)⁷ by means of the Starlink TOPCAT tool using a search radius of 1.5 arcsec, finding 100% match. A morphological type was available for 59 objects (66%). As expected, most of the ELGs are spiral galaxies (43), with a minor fraction of irregular, peculiar or mergers (5 objects). However, a significant fraction of the ELGs (11 sources) are classified as early-type (E to S0) galaxies. The location of the galaxies in projected cluster-centric distance suggests that the morphological transformation from spiral galaxies to S0 occurs *before* the quenching of star formation (Pérez-Martínez et al., in preparation).

Redshift estimates were available for 87 of our ELGs. From these, a vast majority (84) have a redshift close to that of the cluster. There was a re-

⁷<http://www.astro.caltech.edu/~smm/clusters>.

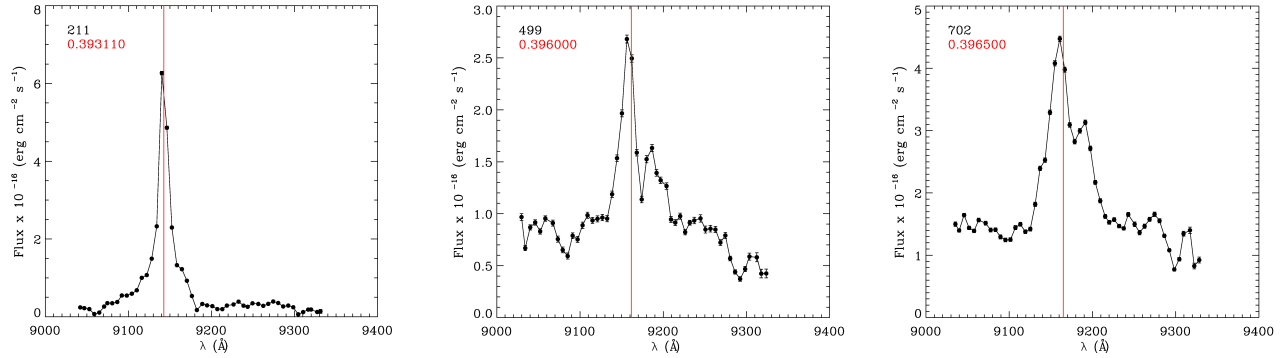


Fig. 1. Examples of pseudo-spectra built from the $H\alpha$ scan (50 steps). Generally one of the N II doublet components is clearly resolved. Spectroscopic redshifts estimates from the public catalogue have been included (vertical line).

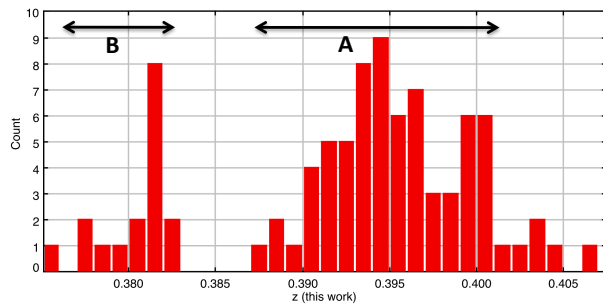


Fig. 2. Distribution of redshifts of ELGs from our narrow-band photometric survey. It is possible to recognize two dynamical structures as in Czoske et al. (2001): structure ‘A’ is the main cluster component, while structure ‘B’ lies along the line of sight to the cluster centre and has been interpreted as an infalling group at high velocity).

markably good agreement between the redshift estimates derived from the position of the $H\alpha$ line within our pseudo-spectra (see redshift lines in Figures 1 and 2) and that derived from spectroscopic measurements. The spatial distribution of the ELG sample, as given by the position of the sources in the sky plane and our redshift estimates, maps the presence of two components: (i) a structure assembling onto the cluster core from the NW with an orientation almost in the plane of the sky. This structure has been already reported by other authors (Moran et al. 2007; Zhang et al. 2005; Kneib et al. 2003). (ii) An infalling group at high velocity nearly along the line of sight to the cluster centre, identified by a double-peaked distribution in the redshift space, as shown in Figure 2 (Moran et al. 2007; Czoske et al. 2001).

The flux completeness limit of the ELG sample, $f(H\alpha) \sim 6.0 \times 10^{-17} \text{ erg s}^{-1} \text{ cm}^{-2} \text{ \AA}^{-1}$ is very well

aligned with the GLACE requirements. The detection density, $\sim 1.4 \text{ arcmin}^{-1}$ is comparable with the average density of other narrow-band surveys (Kodama et al. 2004; Koyama et al. 2011) but the $H\alpha$ fluxes are lower than those reported by Kodama et al. (2004) and therefore the SFR is better aligned with the $(1+z)^6$ evolution prediction mentioned in § 1 above. By means of a $[NII]/H\alpha$ vs. $EW(H\alpha)$ diagnostic diagram (Cid Fernandes et al. 2010), we have obtained a fraction of AGN candidates (Seyfert class) around 20% of ELGs. The fraction over the total number of detections, $\sim 2.5\%$, is larger than that derived from optical spectroscopy ($\sim 1\%$, Dressler et al. 1999) but smaller (around half) than that obtained from X-ray observations (e.g. Koyama et al. 2011).

REFERENCES

- Balogh, M. L., Navarro, J. F., & Morris, S. L. 2000, *ApJ*, 540, 113
- Butcher, H., & Oemler, A., Jr. 1984, *ApJ*, 285, 426
- Cid Fernandes, R., et al. 2010, *MNRAS*, 403, 1036
- Czoske, O., et al. 2001, *A&A*, 372, 391
- Dressler, A., et al. 1999, *ApJS*, 122, 51
- Haines, C. P., et al. 2009, *ApJ*, 704, 126
- Jones, D. H., Shobbell, P. L., & Bland-Hawthorn, J. 2002, *MNRAS*, 329, 759
- Kauffmann, G., et al. 2004, *MNRAS*, 353, 713
- Kennicutt, R. C., Jr. 1998, *ARA&A*, 36, 189
- Kneib, J.-P., et al. 2003, *ApJ*, 598, 804
- Kodama, T., et al. 2004, *MNRAS*, 354, 1103
- Koyama, Y., et al. 2011, *ApJ*, 734, 66
- Miller, C. J., et al. 2003, *ApJ*, 597, 142
- Moran, S. M., et al. 2007, *ApJ*, 671, 1503
- Pereira, M. J., et al. 2010, *A&A*, 518, L40
- Treu, T., et al. 2003, *ApJ*, 591, 53
- Ulmer, M. P., et al. 2009, *A&A*, 503, 399
- Zhang, Y.-Y., et al. 2005, *A&A*, 429, 85